MAGNETIC SUSCEPTIBILITY MAPPING OF ROCKS AND DEPTH ESTIMATION OF ANOMALIES: A CASE STUDY OF IGARRA AND ITS ENVIRONS.

[2]Nwugha V.N., [1] Ikoro D.O, [1]Okeke-Oguegbe C.N [1]Ezebunanwa A.C,

[1] Department of Geology, Federal University of Technology Owerri, Imo State.
[2] Department of Basic Sciences, Alvan Ikoku Federal College of Education Owerri, Imo State.

ABSTRACT

Magnetic Susceptibility Mapping and Depth Estimation of Anomalies were carried out on Igarra and its environs, Southwest Nigeria. This was to assist in mineral exploration in the area. The study area is located within the Igarra schist belt which is underlain by rocks of Precambrian basement complex. The Total Magnetic Field over the study area was obtained by digitizing the aeromagnetic map of Auchi (Sheet 226) acquired from the Nigerian Geologic Survey Agency (NGSA). A total of 19 (nineteen) magnetic anomalies were identified on the map; 5 magnetic highs and 14 lows. 8 anomalies have a NW-SE strike direction, 4 in the NE-SW and 7 in the E-W direction. The amplitude of the anomalies and strength of the total field were used to determine the susceptibility values for each of the anomalies. The Susceptibility values were used to generate a Magnetic Susceptibility map of the study area on SURFER 13 software. TMI plots on the anomalies were carried out on MICROSOFT EXCEL 2010. Depth estimates of the anomalies were got using three methods: The Half Width rule, Hannel rule and Tirburg rule. The Susceptibility map shows a noticeable pattern of increase in magnetic minerals from the Southwestern to the Northeastern part of the map. The Depth of the basement anomalies were relatively shallow ranging from 0.8km to 2.6km. The results of this work provide a preliminary guide to those that engage in mineral exploration / exploitation in the area.

Keywords: Magnetic Susceptibility, Depth, Anomaly, Igarra, Basement, Magnetic intensity

INTRODUCTION

There are several geophysical methods that have since been employed in the investigation of the earth's physical properties and characteristics. Some of them are seismic, electrical, electromagnetic, magnetic and gravity methods. The method to be used for a particular investigation or survey may depend strictly on the nature or purpose of the study. Sometimes, more than one method may be employed to carry out a particular survey. Aeromagnetic method has been widely used since its inception. The most distinguishing feature of this method, compared with other geophysical schemes, is the rapid rate of coverage and low cost per unit

area explored. The use of this method makes it possible for geophysicists to acquire data regardless of ownership or accessibility of remote lands of interest.
This inherent advantage has made it possible for large scale airborne magnetic survey to be carried out around the globe.

Presently, most countries acquire magnetic data to be used both for independent or group studies such as schools or agencies. The government does the regulation through Geological Survey of Nigeria (Now called Nigerian Geological Survey Agency, NGSA), there has been an upsurge of interest in the quantitative and qualitative interpretation of aeromagnetic data. Umera (2011) carried out the interpretation of aeromagnetic data from Ilesha Southwest Nigeria. The results obtained indicate shallow depths to magnetic anomalies. The maximum depth to top of the magnetic source body obtained was 34.2m and minimum depth is 0.5m.Amigun et al (2012) employed the use of airborne magnetic method to explore Ajabanoko iron ore deposit in Okene area of Southwestern Nigeria. The subsurface geology of the deposit province showed relative high magnetic susceptibility (0.016-0.017). Depth estimation is best resolved by ascertaining the shape and size of the anomaly. There are several rule of thumb used in calculating depth to the top of anomaly of which the three reliable and comparable ones were used in this research. The depth to the magnetic sources ranged from 50m to 300m. Chinwuko et al (2014) interpreted aeromagnetic data over Lokoja-Auchi area.The result obtained using the slope methods revealed two depth sources in the study area; on the average the deeper magnetic sources range from 2.3 to 4.9km, while the shallower magnetic sources range from 1.1 to 1.6km. For this study, aeromagnetic data was used to investigate the subsurface properties such as susceptibility distribution and estimation of depth to anomalous features in Igarra area and its environs, South West Nigeria.

Geology of the Area

Geologically, the area of study lies within the Igarra Schist belt (Fig1). The Igarra Schist belt is the eastern most (and perhaps, the best known) formation of the South western Nigeria Schist belts distributed around the Okene magmatic nucleus. The Igarra Schist belt is distinct from other South Western schist belts by the presence of both calcareous rock and conglomerates. The calcareous rocks and conglomerates together with quartzite occurring as bands. Biotite Schist is dominant here, even though gneiss occurs as the margins. This belt and indeed, other schist belts of the Upper Proterozoic formations are generally believed to belong to the Pan African Orogeny (600 ± 150 ma). The geology of Igarra area has been studied at various degrees by many authors. These authors indicate that the major schist (metasediments) occurs as a supracrustal cover on the basement and consists of quartz – Biotite, calc-gneiss and marble, metaconglomerate and mica schist.

Odeyemi (2006), Obaje (2009), Amigun et al (2012), Obasi (2012), Saliu and Komolafe (2014) have discussed the metallogeny of the South-Western Nigerian basement complex and have suggested where exploration might be most effectively directed. Marble occurs within the

Migmatite-gneiss-quatzite complex as relicts of sedimentary units including carbonate rocks. Such marble deposits appear to be limited to the South-western and Central parts of the country (Odeyemi et al, 2006; Obaje, 2009; Obasi, 2012). These authors also confirm the presence of exploitable marble deposits in Igarra area precisely.Probably 90% (Ninety percent) of Nigeria's total gold production of 12,000 (Twelve thousand) kilogram since 1914 has been from alluvial deposits derived from primary gold mineralization (sulphides, galena and pyrite from gold bearing quartz) in the basement rocks. All the producing areas have been in the Western part of the basement where the schist belts are best developed (Obaje, 2009).Amigun et al (2012) identified the presence of iron in Okene province which is part of the Southwestern Nigeria basement complex. Exploitable quantities were also reported to be found in the area by Obaje (2009).Saliu and Komolafe (2014) recorded the presence of exploitable dolomite in Igarra area.

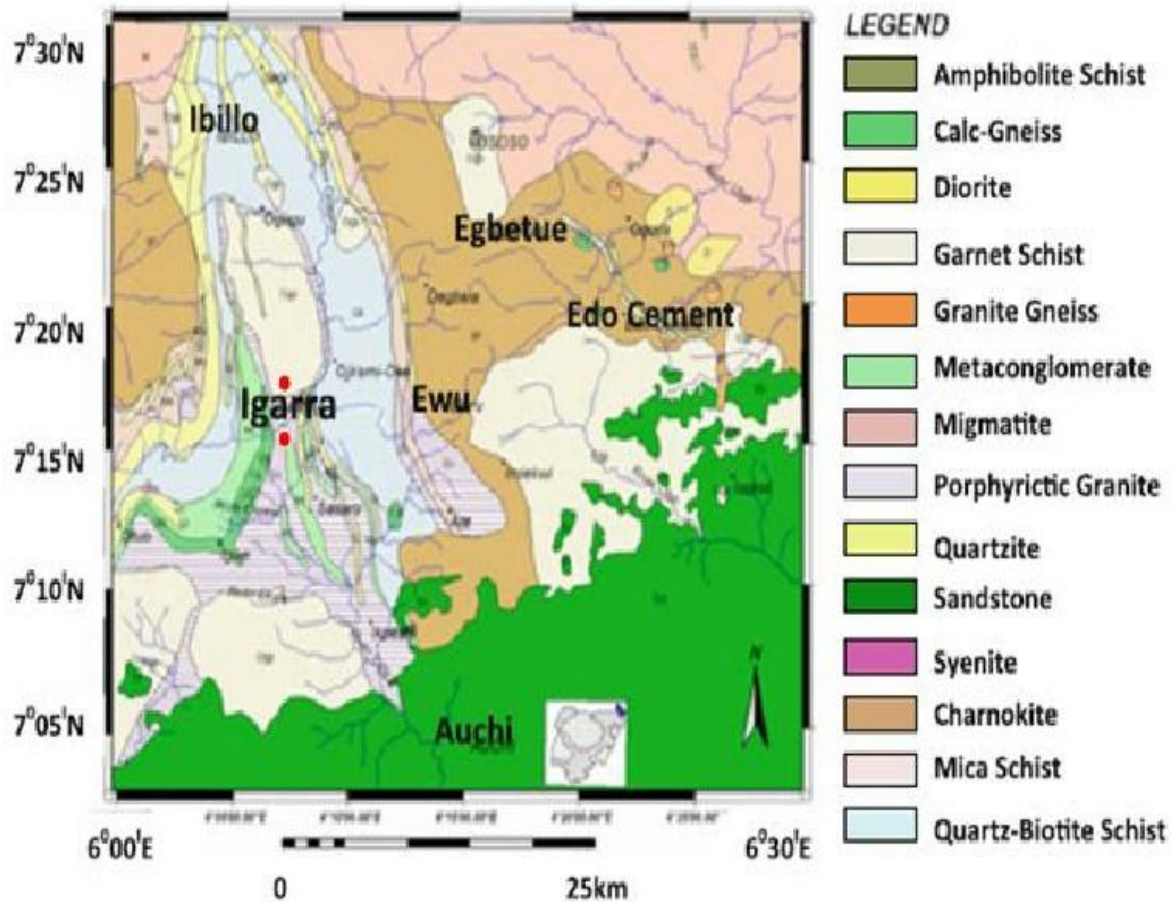

Fig.1. Geologic Map of the study Area (Adapted from Odeyemi, 2009)

MATERIALS AND METHODS

Data acquisition

The aeromagnetic map of Auchi sheet (sheet 226) was acquired from the Nigerian Geological Survey Agency (NGSA). The aeromagnetic data was acquired as the airplane flew along a series of NW-SE flight lines with a nominal flying altitude of 152m (about 500ft) with flight lines spaced 2km in the direction 60/240 (dip/azimuth) degree and contour interval of 20nT. Regional correction was based on International Geomagnetic Reference Field (IGRF) standard. In this study, the digitizing process follows the basic acquired data, analogue flight lines drawn on the map and the obtained data are shown as coloured filled contour maps, Fig. 3. The data was made in form of contoured maps on a scale of 1:100,000.

Susceptibility Distribution

Areas of evident anomalies were identified in the aeromagnetic map of the study area and labelled with numbers, Fig. 2. The contour values were studied to identify whether each area was characterised by either a magnetic high or low. The strike directions of the contours were also identified. For an identified anomaly, the value of the total magnetic intensity about the center was read off and the corresponding value enclosing the anomaly called the host environment (host rock) was measured. The difference between the two gives the amplitude of the anomaly (ΔT). The Total Magnetic Intensity, T was obtained by adding 32,000 nT (Gamma) to the value measured at the center. Susceptibility contrast (ΔK) which is a ratio of change in magnetic intensity to total magnetic intensity of the field, was calculated using the relation:

$$\Delta K = \frac{\Delta T}{2\pi T}$$

Where:

ΔK = Magnetic Susceptibility Contrast

ΔT = Amplitude of the anomaly (Change in magnetic intensity)

T = Strength (magnetic intensity) of the total magnetic field

The susceptibility contrast values for each of the anomalous areas were used as contour values to generate a **susceptibility map (Figures 3 and 4)** for the study area. Figure 3 shows spatial distribution of the magnetic susceptibilities while Figure 4 depicts the models. This is to fully enhance a view of the susceptibility distribution in the study area. The map was contoured manually and was also generated using **Surfer 13 software**.

Depth Estimation

The depth to the top of an anomaly can be estimated using manual or computer aided approach. Any of these methods is called modelling. The modelled anomalies are examined for a parameter of shape that is proportional to the depth. Shape factors measured are the distance over which the slope is maximum, the distance between points where the slope is half of the maximum slope, half the width of the anomaly at half the peak magnitude. Such shape measurements multiplied by index factors give estimates of the depth of the body responsible for the anomaly. Among several rules of thumb developed, Hannel, Tiburg and Half width are related in the method for the depth estimations. Half width rule estimation to the depth of the body is based on the principle that half width between flanks of curves at an amplitude of half the maximum amplitude. Hannel rule of poles estimates depths as half the horizontal distance at 1/3 the maximum amplitude. The Tiburg rule of poles for depth estimation is equal to 2/3 of the horizontal distance between flanks of curves at half the maximum amplitude. All these assume single pole source and of long vertical extent.

After the anomalies were identified, their centers were determined and profiles drawn across each anomaly on the filtered map through a plot of magnetic intensity values, T (gamma) against distances to the center of the anomalies (kilometer). Plots of the profiles were done with requisite softwares (Grapher 6 and **Microsoft Excel 2010).** The determining factor for depth estimation depend on a number of parameters which include; the half slope ($S_{1/2}$) Width between flanks (W), Maximum amplitude (A), Horizontal distance (H) and Point of maximum deflection (PD) of the profiles. The measured parameters are subject to the shape of the generated profiles (curves). These were depending on the shape of the profiles (curves). The basic principle is based on the width of the anomaly and differences in the slopes between their flanks.

RESULTS AND DISCUSSION

Description of the Map

A total of 19 anomalies were identified on the filtered aeromagnetic map of the study area including very small ones with about two contour lines. The underlying metamorphic basement is of non-uniform magnetization. There is variable topography or depth of the anomalies. The major anomalies occur around the Northeastern to Southwestern part of the map with their magnitudes ranging from 32870nT to 33110nT, Figure 2. A set of magnetic highs are located within Latitudes 7.08ºN and 7.48ºN and within Longitudes 6.05ºE and 6.27ºE and these are An3, An6, An10, An12, An13. Magnetic highs also occur at three extreme points of the map (6.5E, 7.0N; 6.5E, 7.5N; 6.0E, 7.0N). The rest of the anomalies are magnetic lows.

The strike directions of the anomalies are as follows:

NW-SE; 8 Anomalies (An2, An3, An4, An5, An6, An9, An14, An15)

NE-SW; 4 Anomalies (An8, An13, An16)

E-W; 7 Anomalies (An1, An7, An10, An12, An17, An18)

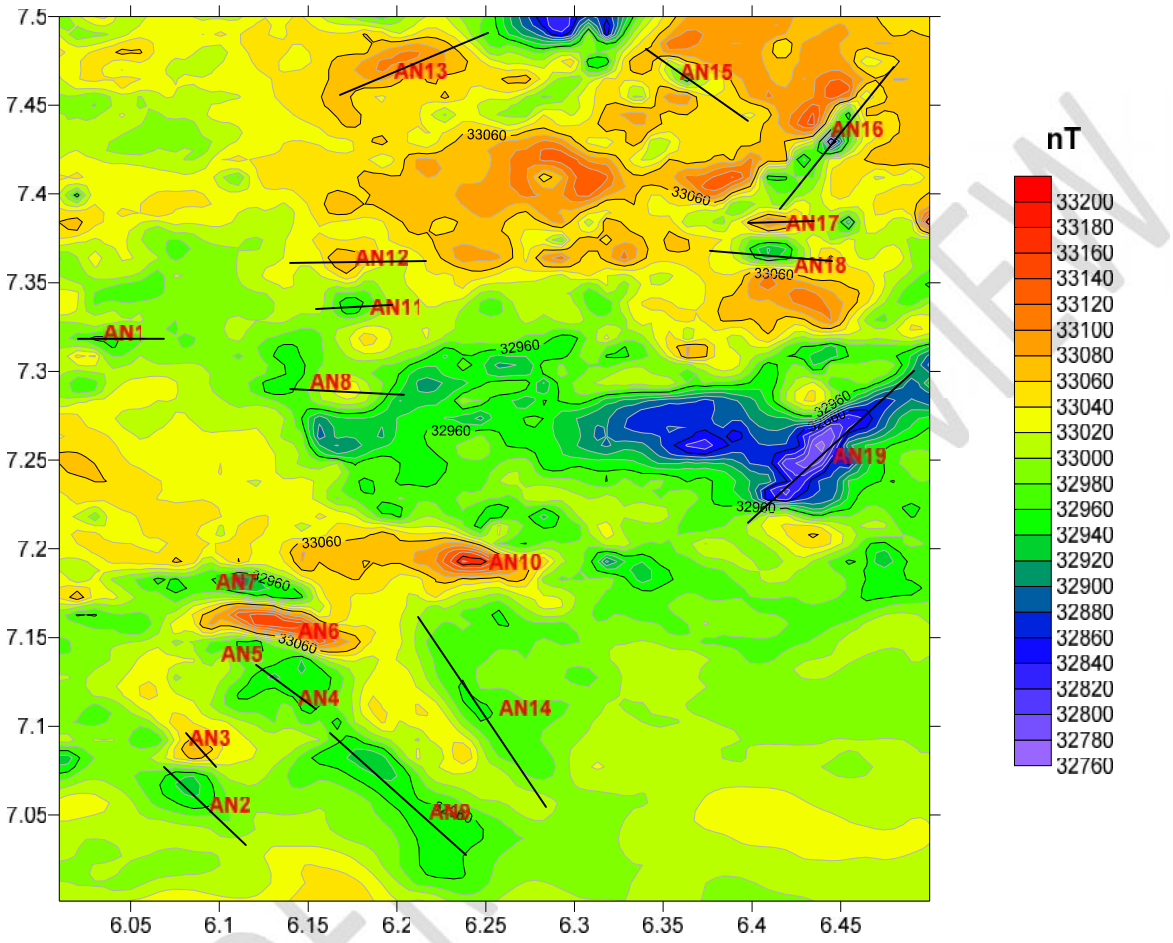

Fig 2: Total Magnetic Intensity Map of Auchi showing Anomalies and their Strike Directions

Susceptibility Distribution

The susceptibility contrast values of the 19 anomalies were calculated including other associated parameters. Table 1 shows strike direction, coordinates and susceptibility contrast (ΔK) which calculated using the relation below with their usual meaning:

$$\Delta K = \frac{\Delta T}{2\pi T}$$

Table 1. Table for Susceptibility Contrast

Anomaly	High or Low	Strike Direction	Coordinates		ΔT	T	$\Delta K \times 10^{-4}$
AN1	L	E-W	E6.0365	N7.3181	40	32960	1.93
AN2	L	NW-SE	E6.0828	N7.0657	50	32960	2.42
AN3	H	NW-SE	E6.0869	N7.0876	50	33060	2.41
AN4	L	NW-SE	E6.1331	N7.1282	30	32960	1.45
AN5	L	NW-SE	E6.1161	N7.1445	30	32960	1.45
AN6	H	NW-SE	E6.1364	N7.1566	80	33020	3.86
AN7	L	E-W	E6.1120	N7.1818	80	32960	3.86
AN8	L	NE-SW	E6.1412	N7.2979	30	32960	1.45
AN9	L	NW-SE	E6.2053	N7.0560	20	32960	0.97
AN10	H	E-W	E6.2378	N7.1932	80	33060	3.85
AN11	L	E-W	E6.1737	N7.3384	30	32960	1.45
AN12	H	E-W	E6.1704	N7.3628	30	33060	1.44
AN13	H	NE-SW	E6.1997	N7.4764	60	33060	2.89
AN14	L	NW-SE	E6.2419	N7.1136	20	32960	0.97
AN15	L	NW-SE	E6.3628	N7.4650	90	32960	4.35
AN16	L	NE-SW	E6.4448	N7.4293	140	32960	6.76
AN17	L	E-W	E6.4107	N7.3839	60	33000	2.9
AN18	L	E-W	E6.4099	N7.3677	60	32960	4.83
AN19	L	NE-SW	E6.4391	N7.2581	90	32860	4.36
EXTREME POINTS	H		E6.5000	N7.0000	30		1.45
	H		E6.5000	N7.5000	20		0.97
	L		E6.0000	N7.5000	20		0.99
	H		E6.0000	N7.0000	30		1.45

Within Latitudes 7.15N and 7.20N and Longitudes 6.10E and 6.20E which is at Igarra, a high susceptibility value of 3.86 $\times 10^{-4}$ occurred around anomalies 6 and 7; the high susceptibility value agrees with the granitic rocks around the area, Figure 3. A lower susceptibility value of 1.45 $\times$ 10^{-4} occurred around anomalies 4 and 5 which are below the previous two. The variation in susceptibility values around this area may be due to the nature of the intrusives in the area. Within Latitudes 7.0N and 7.15N and Longitudes 6.15N and 6.3N which is at Auchi area, a low susceptibility value of 0.97 $\times$ 10^{-4} occurred around anomalies 9 and 14; the low susceptibility value agrees with the cretaceous sediments around the area. The susceptibility map reveals that the rock susceptibilities of the study area have a definite trend in the distribution of magnetic materials. There is a noticeable pattern of increase from the Southwestern part of the map towards the Northeastern part of the map. The areas of high susceptibility values can be differentiated easily from areas of low susceptibility in the three dimensional view, Figures 4 and 5. The contrast shows the presence of magnetic rocks which may be the reason for the anomalies observed within the study area.

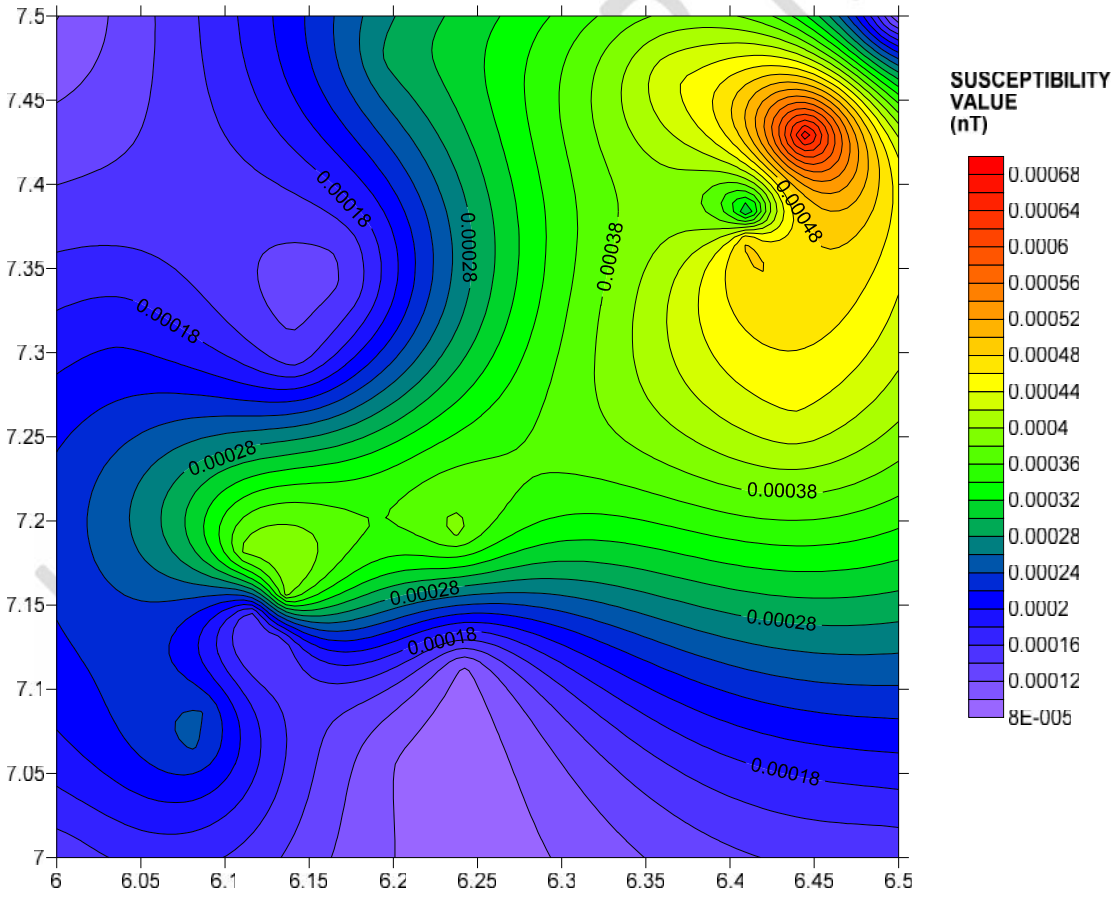

Figure 3: Magnetic Susceptibility map of the Study Area Showing Rock Contrasts

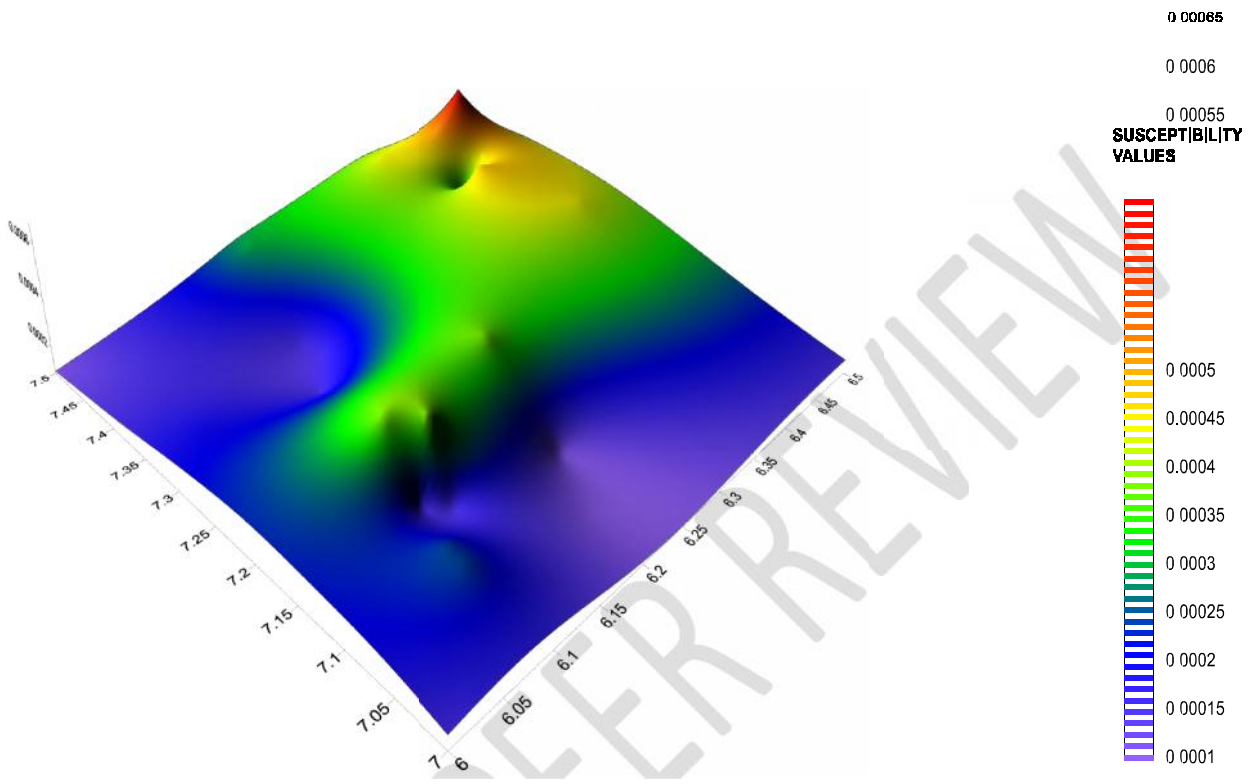

Figure 4: Three Dimensional View of the Magnetic Susceptibility Distribution in the Area

Depth Estimation of the Observed Anomalies

The depths of the observed anomalies were got by a plot of TMI against Distance for all the anomaly profiles. Profiles were drawn from the center to right and left of the anomaly which is perpendicular to the strike of the anomaly, Nwugha (2000). This was done for the respective anomalies and curves drawn to determine the half slope ($S_{1/2}$), Width between flanks (W), Maximum amplitude (A), Horizontal distance (H), Point of maximum deflection (PD) and hence estimation of the depths to the anomalies, Adarighofua (2014).

The three rules of thumb; half width rule, Hannel rule and Tiburg rule were most suitable for the parameters measured on each of the profiles (curves) .Figures (5.1. and 5.2) are examples of shapes of with low magnetic intensities while Figures (5.3 and 5.4) represent anomalies with high magnetic intensities. They were compared to adequately identify the approximate depth to anomalies in the study area. Table 2 shows the estimated depth to anomaly.

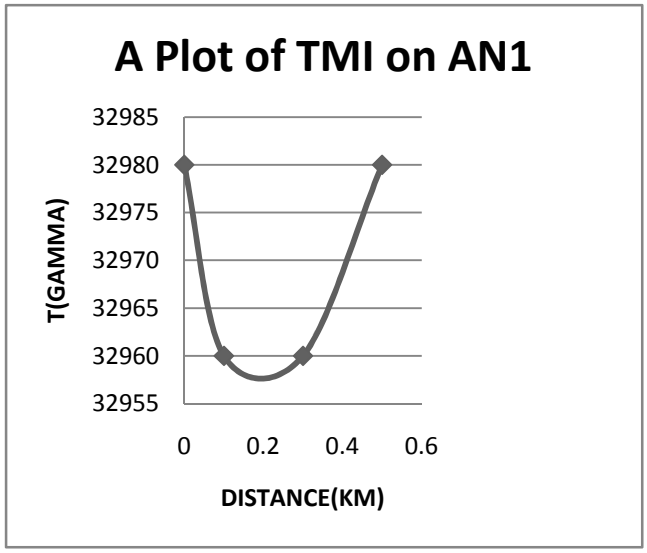

Figure 5.1: Magnetic intensity against Distance of Anomaly 1.

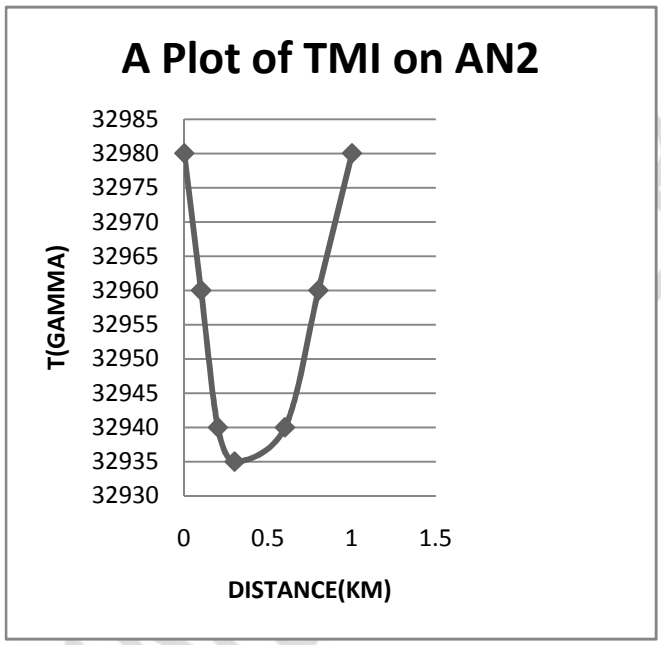

Figure 5.2:Magnetic intensity against Distance of Anomaly 2

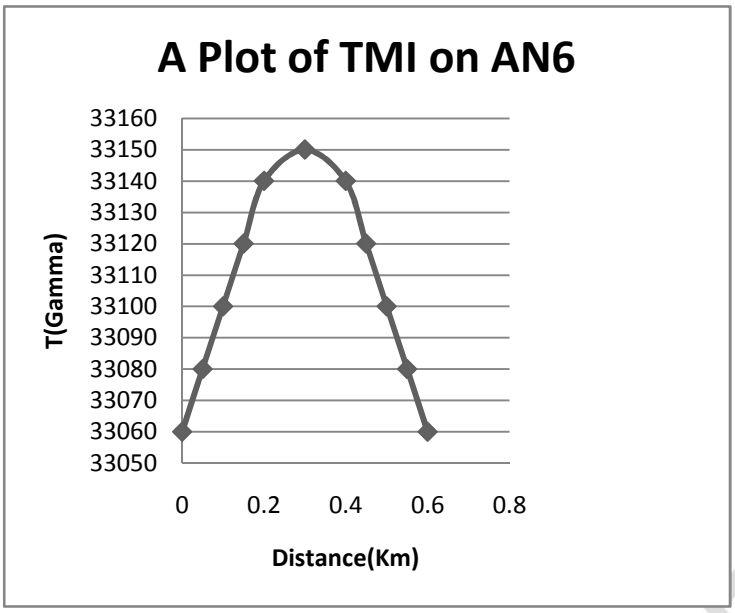

Figure 5.3: Magnetic intensity against Distance of Anomaly 6

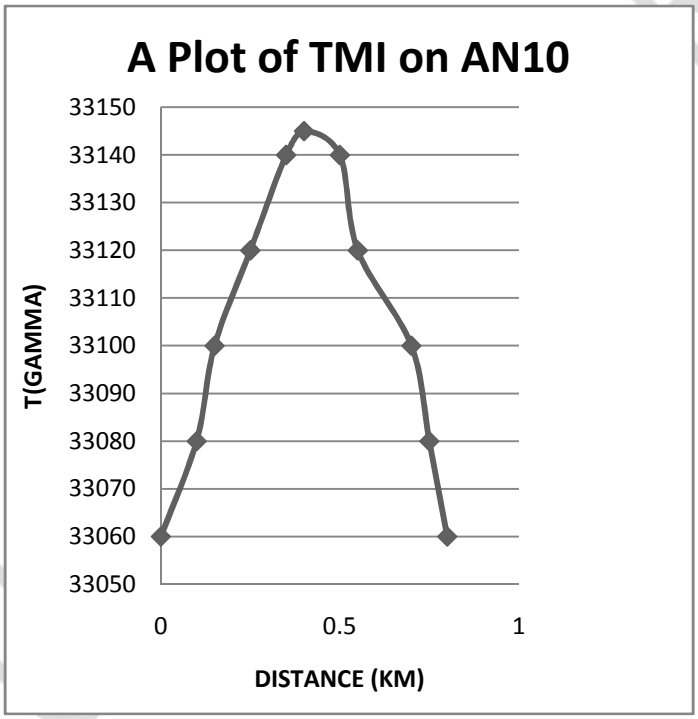

Figure 5.4: Magnetic intensity against Distance of Anomaly 10

Table 2: Estimation of Depth using three depth estimation methods

Anomaly	Half Width (1/2W@1/2A)	**Hannel Rule (1/2H @1/3A)**	Tirburg Rule (2/3H@1/2A)	Approx. Depth
AN1	1.6km	1.7km	2.1km	1.8km
AN2	1.2km	1.3km	1.6km	1.4km
AN3	1.4km	1.7km	1.8km	1.6km
AN4	2.0km	2.1km	2.6km	2.2km
AN5	1.7km	1.8km	2.2km	1.9km
AN6	1.2km	1.5km	1.6km	1.4km
AN7	1.3km	1.5km	1.7km	1.5km
AN8	1.5km	1.8km	2.0km	1.8km
AN9	1.2km	1.4km	1.5km	1.4km
AN10	1.5km	1.7km	2.0km	1.7km
AN11	1.6km	1.8km	2.1km	1.8km
AN12	1.8km	2.1km	2.4km	2.1km
AN13	1.6km	1.9km	2.1km	1.9km
AN14	0.9km	1.3km	1.2km	1.1km
AN15	1.7km	2.1km	2.3km	2.0km
AN16	0.8km	1.1km	1.1km	1.0km
AN17	1.2km	1.7km	1.5km	1.5km
AN18	1.2km	1.6km	1.5km	1.4km
AN19	1.8km	2.2km	2.4km	2.1km

A general view of the depth calculations show that the anomalies are not deeply buried. The shallowest depth to the top of anomaly is approximately 0.8km while the deepest is approximately 2.6 km. This agrees with the depth estimate given by Chinwuko et al (2014).

Structural Trends and fault location

The strike directions of the identified anomalies trend in the NE-SW, NW-SE and E-W with dominant trend in the NW-SE directions, Figure 6, Table 3. The strike directions correspond with the findings of Kehinde et al (2013); Adiela and Ofuyah (2017).

A fault is expected to run in the North – South direction of the map through anomalies 4, 5, 7, 9 and through anomalies 15, 16, 17, 18, 19. This is because a series of closed lows on the map suggests the location of fractures or possible faults (Reeves, 2005). At the Southeastern part of the map, faults are expected to run through anomalies 12, 16, 17 and 18 with an East-West trend. This is because a series of continuous gap between major anomalies in the map shows possible fault areas (Nwugha, 2000). The trend and pattern of faults in the area agrees with the findings of Oden (2014), Akperi et al (2016) andUdinmwen et al (2016).

Table 3: Frequency distribution of anomalies / strike direction

Strike Direction	No of Anomalies
E-W	7
NW-SE	8
NE-SW	4

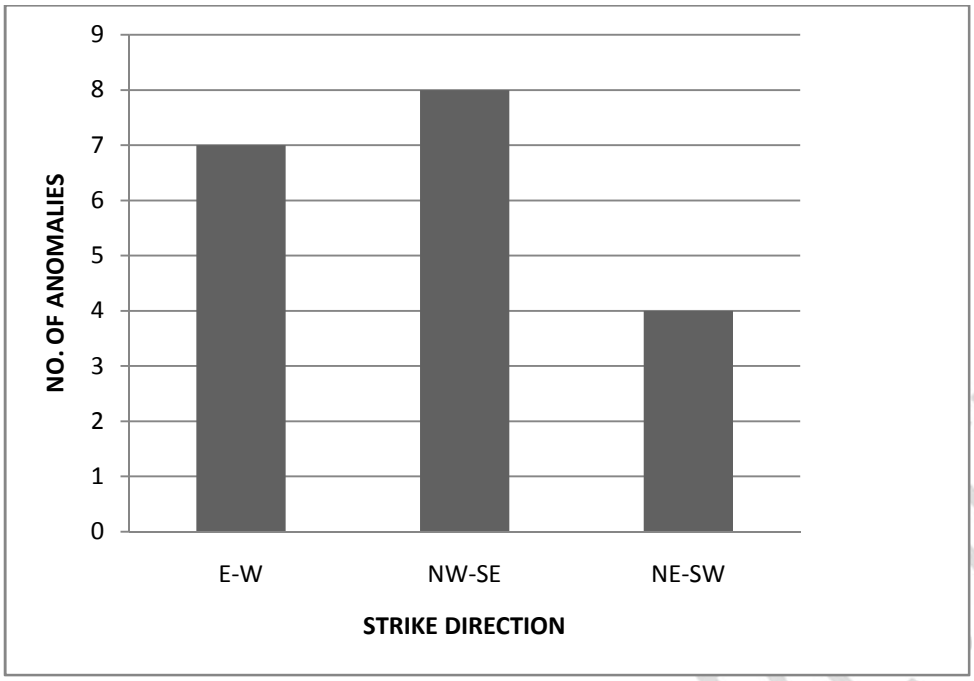

Figure 6: Bar chart showing No. of Anomalies/strike direction

CONCLUSION

About Nineteen anomalies were identified within the study area. Within the Southwestern parts of the map around Latitudes 7.0N and 7.15N and Longitudes 6.15N and 6.3N (Auchi area), a low susceptibility contrast occurred which agrees with the cretaceous sediments, mainly sandstones found around the area. A series of closed lows on the map suggests the location of fractures or possible faults (Reeves, 2005).The susceptibility map reveals that the rock susceptibilities of the study area have a definite trend in the distribution of magnetic materials. There is a noticeable pattern of increase from the Southwestern part of the map towards the Northeastern part of the map.Going with the susceptibility distribution in the area, which is from Southwestern towards the Northeastern part, sediments are expected to occur dominantly within the Southwestern part; while igneous and metamorphic rocks are expected to be dominantly within the Northeastern part.Within the igneous rocks, the mafic types are expected to tend more towards the Northwestern part while the felsic types are expected to tend more towards the Southwestern direction. This is because mafic igneous rocks are more magnetically susceptible than the felsic igneous rocks due to their mineral content (Reeves, 2005).The depth of the basement anomalies are in the range of 0.8Km to 2.2Km. The depth of the anomalies increases with their widths

REFERENCES

Adarighofua M.O.(2014). Independent Geologic Field Mapping of the Igarra Axis of the Basement Complex and Benin Flank of Anambra Basin in Northern Part of Edo State. An unpublished field mapping report submitted to Department of Earth Sciences, FUPRE, Delta State.

Adiela U.P. and Ofuyah W.N. (2017).The Structural Geology of Eshiawa in Igarra Area, Southwestern Nigeria. Journal of Scientific and Engineering Research, 2017, 4(4):273-282.

Akperi G. O., Osagiede E. E. and Ogbamikhumi A. (2016). Fracture analysis of the Basement Complex Rocks in Igarra and Environs, Edo State. Programme and Book of Abstracts, 52nd Annual International Conference of Nigerian Mining and Geosciences Society (NMGS).

Alu, O.O and Mustapha, M. (2015).Interpretation of Aeromagnetic Data of Parts of Share for Geotechnical Studies Sheet 202, South-Western Nigeria. A Paper Presented at the 52nd Annual International Conference and Exhibitions of Nigerian Mining and Geosciences Society, Ilorin 2015.

Amigun J. O., Afolabi O. and Ako B.D. (2012).Application of Airborne Magnetic Data to Mineral Exploration in the Okene Iron ore Province of Nigeria. International Research Journal of Geology and Mining.2(6), pp.132-140.

Chinwuko A. I., Usman A. O., Onwuemesi A. G., Anakwuba E. K., Okonkwo C. C., Ikumbu E. B. (2014). Interpretations of Aeromagnetic Data OverLokoja and Environs, Nigeria. International Journal of Advanced Geosciences, 2(2), pp. 66-71.

Kearey P., Brooks M., Hill I. (2002). An Introduction to Geophysical exploration. Blackwell Science Limited United Kingdom.Pp 155-181.

Kehinde I. O., Ukaegbu V.U., Omosanya K. O., Ideozu R. U. and Mosuro G.O. (2013).Geological and Geophysical Mapping of Fracture Anisotropy at Aiyegunle and Environs, Igarra Area, Southwestern Nigeria.Journal of Geology and Mining Research.5(3), pp.65-74.

Milsom J. (2003). Field Geophysics. John Wiley and Sons Ltd, England. Pp 51-67.

Nwugha V. N. (2000). A Qualitative Interpretation of Takum (Sheet 273) Through Image-Based Display and Depth Calculations.An unpub.Msc. Thesis submitted to the Department of Geology, Federal University of Technology, Owerri.

Obaje N. G. (2009). Geology and Mineral Resources of Nigeria. Lecture Notes in Earth Sciences 120. Springer Dordrecht Heidelberg London, New York. Pp.13-30, 117-154.

Obasi R. A.(2012). Geochemistry and Appraisal of the Economic Potential of Calc-gneiss and Marble from Igarra, Edo State, Southwest, Nigeria.ARPN Journal of Science and Technology. 2(10), pp 1018-1020.

Oden I. (2014). Fracture Characterization, Mineral Vein Evolution and the Tectonic Pattern of IgarraSyn-Tectonic Granite, Southwestern Nigeria. British Journal of Applied Science and Technology.4(17), pp 2417-2429.

Odeyemi I. B. (2006). The Ifewara Fault in Southwestern Nigeria: Its Relationship with Fracture Zones along the Nigerian Coast. Center for Geodesy and Geodynamics, Toro, Bauchi State.Pp 1-13.

Reeves, C. (2005). Aeromagnetic Survey: Principles, Practice and Interpretation. Earth-works, Washington D.C.

Saliu M.A. and Komolafe K. (2014). Investigating the Effect of Dolomite Exploitation on Groundwater Condition of Ikpeshi, Akoko-Edo, Edo State.

Udinmwen E., Oden M.I., Ayuba R., Asinya A. E. (2016). Structural Control on Mineral Vein Geometry in the Igarra Schist Belt, Southwestern Nigeria.Journal of Earth and Atmospheric Sciences. 1(1) pp. 10-21.

Umera, R.B. (2011). Interpretations of Aeromagnetic Data from Ilesha, Southwest Nigeria.An Unpub.Msc Thesis submitted to the Department of Geology, University of Nigeria, Nsukka.